

A Low-Cost Wideband Quasi-Yagi SIW-Based Textile Antenna

Mir Emad Lajevardi^{1, *} and Manouchehr Kamyab²

Abstract—A low-cost wideband textile antenna based on the substrate integrated waveguide (SIW) technology is proposed, and a pure copper taffeta fabric etched on a woolen felt substrate is used to realize the presented antenna. The impedance matching frequency band for the designed structure is from 2.27 GHz to 3.61 GHz which is significantly improved compared with previous studies. The operational principle of the proposed quasi-Yagi textile antenna is also described in this paper. The antenna is fabricated and measured, and a good agreement is achieved between the simulation and experimental results. The designed antenna has the maximum gain and efficiency of 4.2 dB and 84%, respectively. According to its compactness, low-cost and low-weight specifications, the proposed antenna is a good candidate for being utilized in wearable communication devices.

1. INTRODUCTION

Electromagnetic wearable devices such as smart glasses have attracted great attention, especially in recent years [1]. Due to the high permittivity of the human body, its effects should be considered during the design of wireless body area networks antennas [2]. Thereupon, it is required for such lightweight, low-cost and compact structures to have their radiation performance preserved even in the presence of the human body. In addition, due to destructive thermal effects of antennas, it is avoided to locate the antenna near the human body. Utilizing substrate integrated waveguide (SIW) technology increases the isolation of the wearer and antenna without the need for a large ground plane [3]. To the best of the authors' knowledge, only a few studies have dealt with wideband SIW-based textile antennas [4–7].

In this paper, a wideband SIW-based antenna is designed using the textile materials for wearable communication devices. The structure is composed of microstrip line feed, SIW to coplanar SIW (CPS) transition and an antipodal dipole element. Considering the semi-Yagilike structure, the operating frequency band for the designed structure is from 2.27 GHz to 3.61 GHz. The performance is substantially improved compared with previous studies in terms of frequency bandwidth. According to its lightweight, compactness and low-cost characteristics, this structure is a good candidate for wearable applications such as handbag, backpack, jacket and gloves.

2. ANTENNA DESIGN

A parasitic linear array of parallel dipoles is called a Yagi-Uda antenna, which is commonly known as Yagi antenna. Yagi-Uda antennas are very popular because of their simplicity [8]. A woolen felt material with the thickness of $h = 3$ mm, dielectric permittivity of $\epsilon_r = 1.4$ and loss tangent of $\tan(\delta) = 0.025$ is used as the substrate of proposed antenna. The dielectric parameters of the textile material are extracted from the matrix-pencil two-line approach and the method proposed in [9] is used for determining the substrate permittivity. Electron conductive fabric textile with the thickness

Received 4 January 2017, Accepted 31 March 2017, Scheduled 14 April 2017

* Corresponding author: Mir Emad Lajevardi (st_e_lajevardi@azad.ac.ir).

¹ Department of Electrical Engineering, South Tehran Branch, Islamic Azad University, Tehran, Iran. ² Department of Electrical and Computer Engineering, K. N. Toosi University of Technology, P. O. Box 16315-1355, Tehran, Iran.

of $80\ \mu\text{m}$ and surface resistance of $R_s = 0.05\ \Omega/\text{sq}$ has been established on both sides of the structure. A microstrip to SIW transition is designed by means of the parallel half-mode substrate integrated waveguide (HMSIW). In the fundamental-mode, the designed transition has better matching properties than the conventional ones. The structure is also composed of three parasitic elements, which act as antenna directors. These directors not only increase the antenna gain, but also play an important role to achieve wideband properties. Due to various current paths at different frequencies, in order to improve the frequency bandwidth, a bow-tie structure is utilized. All the procedures of antenna design are implemented using full-wave CST Microwave Studio 2016 [10].

3. MANUFACTURING PROCEDURE

First, the designed layout is cut using a scalpel. Then, by using an adhesive, both conductive textiles of top and bottom layers are attached to the antenna substrate. The diameters of the vias inserted by brass eyelets are selected as $d = 3.07\ \text{mm}$ and the space of via centers are $s = 6\ \text{mm}$. This issue causes

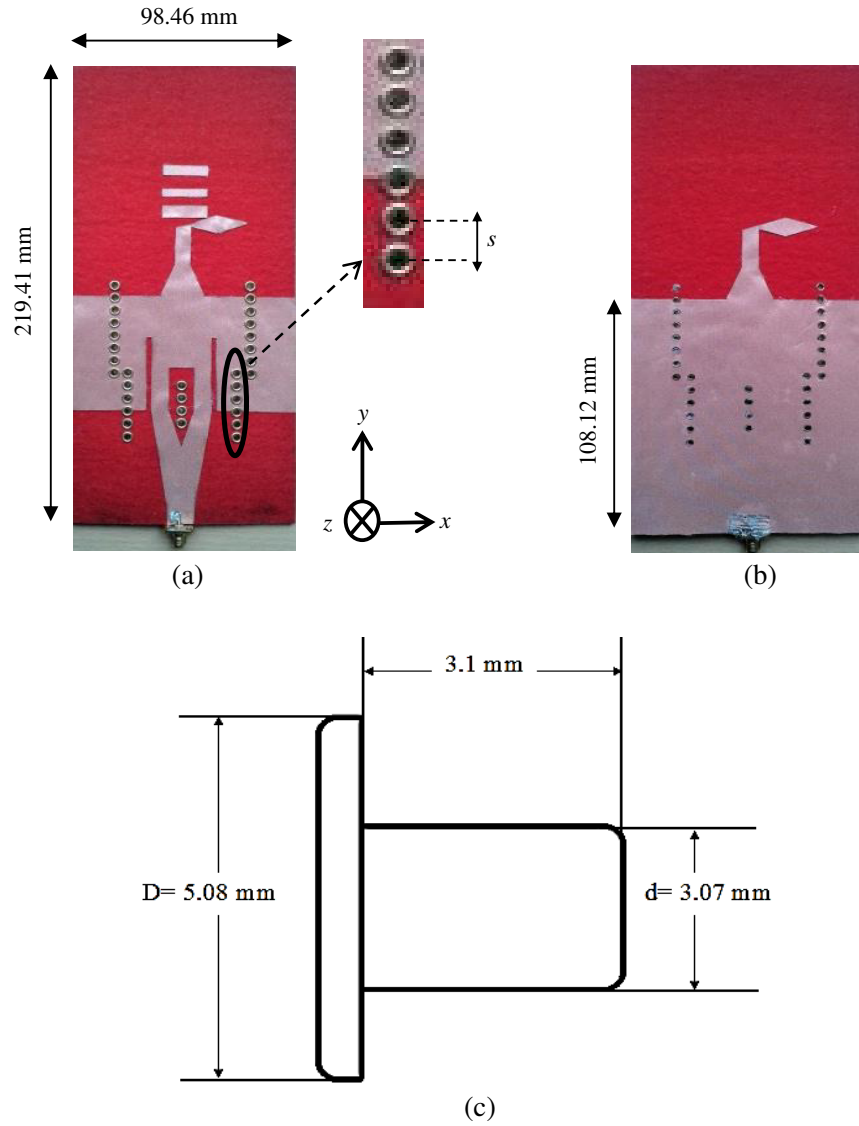


Figure 1. Fabricated prototype of the textile SIW-based antenna. (a) Top view. (b) Bottom view. (c) Front view of brass eyelet.

a wearable capability and flexible performance for the proposed antenna. These brass eyelets have the flange diameter of $D = 5.08$ mm that is considered in our simulations. So, the reflection coefficient of the antenna does not shift forward. This brass eyelet is depicted in Figure 1(c). Eventually a $50\ \Omega$ SMA port is connected to the upper layer. Conductive textile Flectron has good resistance against soldering. Finally, the photograph of fabricated antenna is illustrated in Figures 1(a), (b).

4. EXPERIMENTAL RESULTS

The reflection coefficient of the antenna versus frequency is measured in an anechoic chamber using an Agilent E8361C PNA Microwave Network Analyzers can be seen in the measurement setup in Figure 2. Figure 3 also shows the simulation and experimental results for the reflection coefficient of the proposed

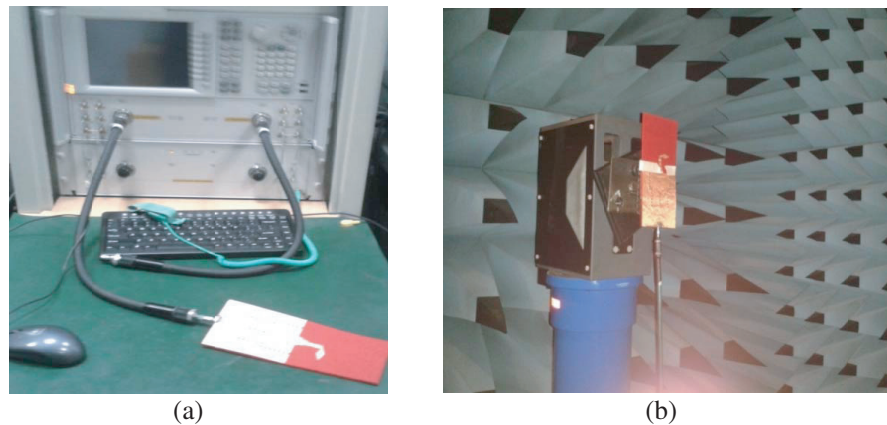


Figure 2. Measurement setup for the proposed antenna. (a) Measurement S_{11} by network analyzer. (b) Radiation pattern in the anechoic chamber.

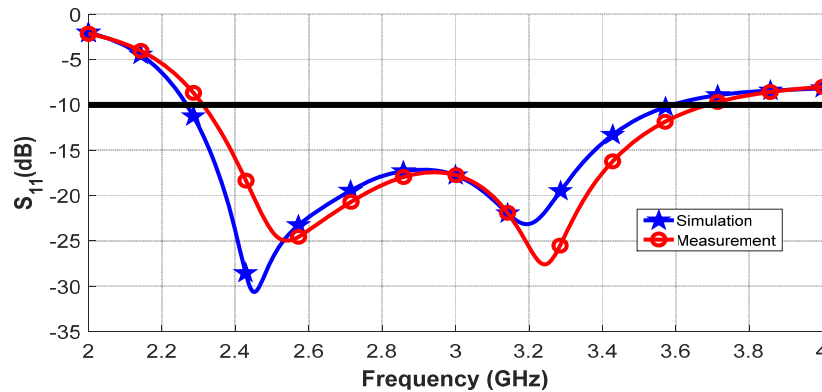


Figure 3. Comparing the simulated and measured reflection coefficient curves of the antenna.

Table 1. Simulated (measured) characteristics of the antenna.

f (GHz)	Gain (dB)	FTBR (dB)	Half-power beamwidth (deg)	
			H -plane	E -plane
2.4	3.3 (3.4)	11.7 (6.8)	184.5 (180.6)	56.7 (61.0)
3.0	3.9 (4.2)	7.1 (5.2)	189.4 (174.6)	60.6 (67.2)
3.6	3.8 (3.7)	7.7 (6.6)	191.1 (184.3)	58.7 (70.80)

antenna. As can be seen, a good agreement between the simulation and measurement results is observed. An impedance matching frequency bandwidth with the reference impedance of $Z = 50 \Omega$ is obtained from 2.31 GHz to 3.69 GHz results in a fractional bandwidth of 46% ($BW = 1.38$ GHz). Therefore, the antenna shows a wideband behavior and its reflection coefficient is better than 5 dB from 2.19 GHz to 4 GHz. The measured results show that a slight upward frequency shift occurs which maybe is due to the imperfect connection between the connector and the antenna as well as the dispersive behavior of woolen felt material.

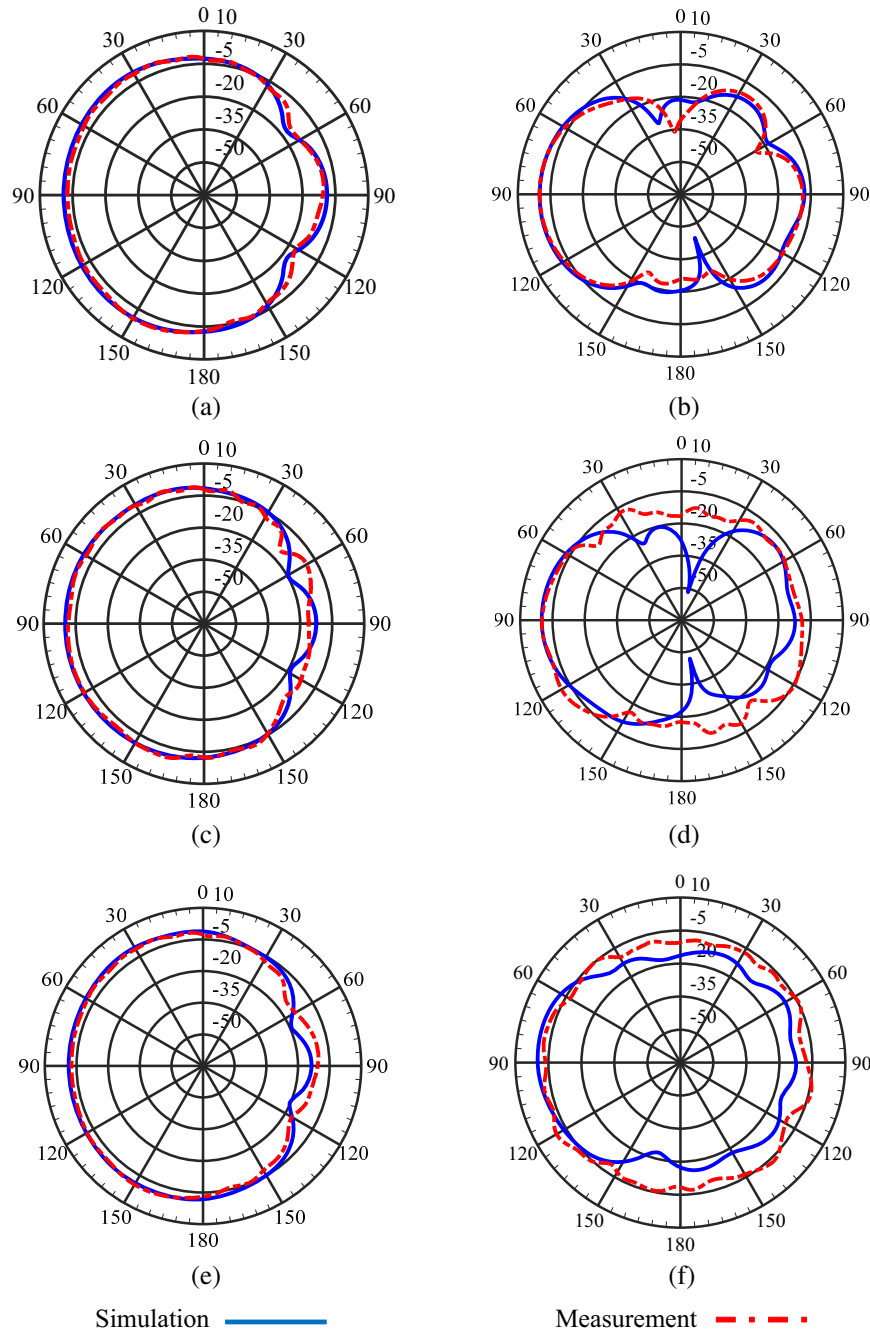


Figure 4. Normalized simulated and measured radiation patterns [dB] of the antenna: (a) $\varphi = 90^\circ$ at 2.4 GHz in H -plane; (b) $\theta = 90^\circ$ at 2.4 GHz in E -plane; (c) $\varphi = 90^\circ$ at 3.0 GHz in H -plane; (d) $\theta = 90^\circ$ at 3.0 GHz in E -plane; (e) $\varphi = 90^\circ$ at 3.6 GHz in H -plane; (f) $\theta = 90^\circ$ at 3.6 GHz in E -plane.

According to the antenna orientation shown in Figure 1, the electric field is directed along the x direction. The simulated and measured radiation patterns of this antenna along the endfire in the E - and H -planes at 2.4 GHz, 3.0 GHz and 3.6 GHz are demonstrated in Figures 4(a)–(f). This figure illustrates that the simulated and measured results are in a good agreement. The other parameters such as antenna gains, front to back ratio (FTBR) and 3-dB beamwidth at E - and H -planes are also simulated, measured and given in Table 1. The measured gain at 2.4 and 3.0 GHz is slightly higher than the simulated one, whereas the gain at 3.6 GHz is less. As represented in this table, the antenna gain at 2.4 GHz, 3.0 GHz and 3.6 GHz is averagely around 3.7 dB. The measured 3-dB beamwidth along the H -plane is narrower than that of simulation. As the frequency increases, the measured 3-dB beamwidth along the E -plane is also increased.

In order to evaluate the effects of the absorbed radiation on the human body, specific absorption

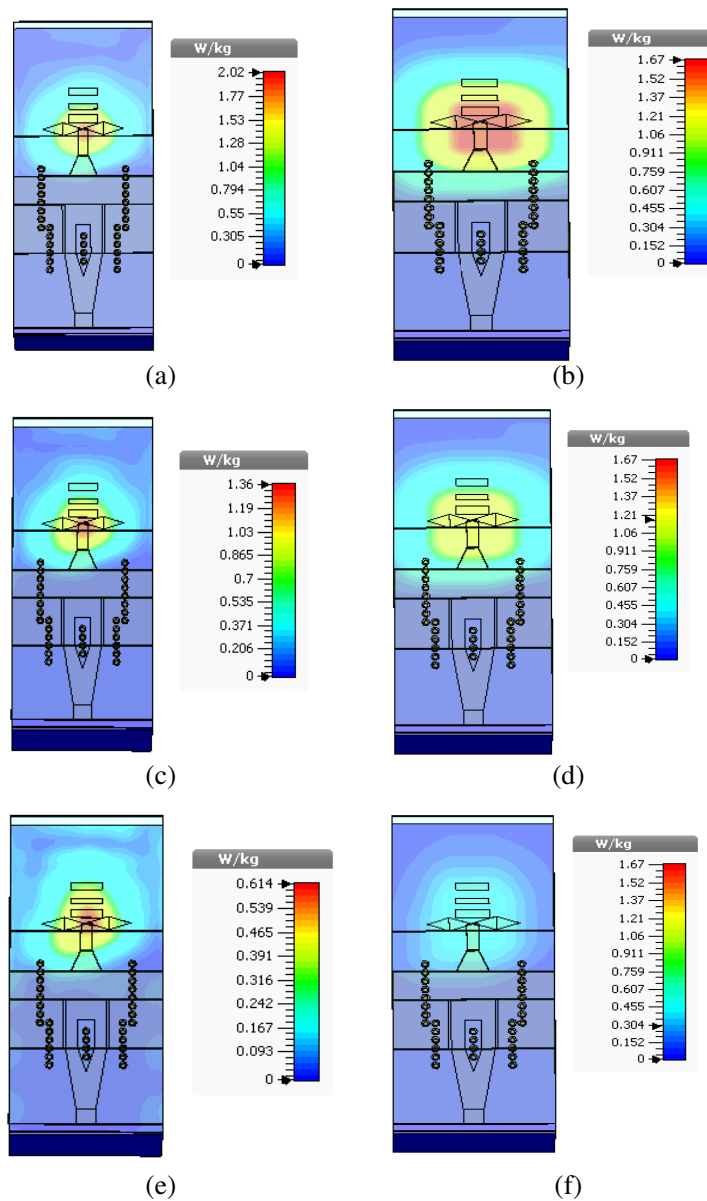


Figure 5. The SAR distribution at various frequencies in 1 and 10 g tissues: (a) 2.4 GHz in 1 g tissue; (b) 2.4 GHz in 10 g tissue; (c) 3.0 GHz in 1 g tissue; (d) 3.0 GHz in 10 g tissue; (e) 3.6 GHz in 1 g tissue; (f) 3.6 GHz in 10 g tissue.

rate (SAR) values are simulated at various frequencies. The SAR is defined as the power absorbed per unit mass of the tissue:

$$\text{SAR} = \frac{d}{dt} \left(\frac{dW}{\rho \cdot dV} \right) \left(\frac{\text{W}}{\text{kg}} \right)$$

in which ρ is the mass density, W the energy absorbed by the human tissue and V the volume of the studied sample.

The antenna is placed at 15 mm distance from a three layered human body model in a 1 g and 10 g tissue. This three-layered model includes of a 3 mm thick skin, 7 mm thick fat and 60 mm thick muscle [11]. Figure 5 demonstrates the calculated SAR distribution for 1 g and 10 g tissues at three different frequencies in the considered frequency band. By supplying 0.5 W (rms) power to the input port, the SAR values over 10 g of the human tissue, are calculated according to IEEE C95.3 standard which is 1.67 W/kg at 2.4 GHz, 1.17 W/kg at 3.0 GHz and 0.29 W/kg at 3.6 GHz on average. These values are less than the average of 2 W/kg introduced by the European standards. In addition, the average SAR values over 1 g of the human tissue, are computed as 2.02 W/kg, 1.36 W/kg and 0.614 W/kg at 2.4, 3 and 3.6 GHz, respectively. The calculated values at 3.0 and 3.6 GHz are below the American and Canadian limits of 1.6 W/kg on average. To obey the SAR limits, the input power to the antenna should be less than 0.4 W (rms) at 2.4 GHz. According to the results, it is recommended to use this antenna for wearable applications like jackets, i.e., direct contact with the human body should be prohibited.

At the end, a comparison between the performances of the proposed antenna and previously reported structures is carried, out and the corresponding results are given in Table 2.

Table 2. Comparing the frequency bandwidth, gain and efficiency of previous results and the proposed structure.

Reference	Fractional bandwidth	Gain (dBi)	Efficiency
Ref. [7]	15%	5.1	92%
Ref. [6]	24%	4.3	85%
Ref. [5]	33%	6.8	-
Ref. [4]	34%	4.0	-
Proposed work	46%	4.2	84%

5. CONCLUSIONS

A wideband low-cost wearable antenna based on the substrate integrated waveguide technology and fully textile material was manufactured. This antenna was operated in a wideband frequency range from 2.31 GHz to 3.69 GHz (BW = 46%) including ISM, WIMAX, Bluetooth, RFID system and military bands. The mechanism of the investigated quasi-Yagi textile antenna was discussed in the paper. The antenna was fabricated and measured and a good agreement was obtained between the simulation and experimental results. The designed antenna had the maximum gain and efficiency of 4.2 dB and 84%, respectively. Considering its compactness, low cost and low weight, the proposed antenna has practical potentials for being utilized in wearable communication devices.

ACKNOWLEDGMENT

We would like to thank the staff of Antenna Laboratory, University of Tehran because of their efforts for the experimental results.

REFERENCES

1. Hall, P. S., et al., "Antennas and propagation for on-body communication systems," *IEEE Antennas Propag. Mag.*, Vol. 49, No. 3, 4158, Jun. 2007

2. Hong, Y., J. Tak, and J. Choi, "An all textile SIW cavity-backed circular ring slot antenna for WBAN applications," *IEEE Antennas and Wireless Propagation Letters*, Vol. 15, 1995–1999, Apr. 2016.
3. Agneessens, S. and H. Rogier, "Compact half diamond dual-band textile HMSIW on-body antenna," *IEEE Transactions on Antennas and Propagation*, Vol. 62, No. 5, 2374–2381, May 2014.
4. Castel, T., S. Lemey, P. Van Torre, C. Oestges, and H. Rogier, "Four-element ultra-wideband textile cross array for dual spatial and dual polarization diversity," *IEEE Antennas and Wireless Propagation Letters*, Vol. 16, 481–484 June. 2016.
5. S. Lemey and H. Rogier.: "SIW textile antennas as a novel technology for UWB RFID tags," *RFID Technology and Applications Conference (RFID-TA)*, 256–260, Sept. 2014.
6. Caytan, O., S. Lemey, S. Agneessens, D. V. Ginste, P. Demeester, C. Loss, R. Salvado, and H. Rogier, "Half-mode substrate-integrated-waveguide cavity-backed slot antenna on cork substrate," *IEEE Antennas and Wireless Propagation Letters*, Vol. 15, 162–165, May 2016.
7. Lemey, S., F. Declercq, and H. Rogier, "Dual-band substrate integrated waveguide textile antenna with integrated solar harvester," *IEEE Antennas and Wireless Propagation Letters*, Vol. 13, 269–272, Jan. 2014.
8. Stutzman, W. L. and G. A. Thiele, *Antenna Theory and Design*, 166–175, John Wiley & Sons, May 2012.
9. Declercq, F., H. Rogier, and C. Hertleer, "Permittivity and loss tangent characterization for garment antennas based on a new matrix-pencil two-line method," *IEEE Transactions on Antennas and Propagation*, Vol. 56, No. 8, 2548–2554, Aug. 2008.
10. Computer Simulation Technology (CST), ver. 2016, [Online], Available: <http://www.cst.com>.
11. Yan, S., P. J. Soh, and G. A. E. Vandebosch, "Dual-band textile MIMO antenna based on substrate-integrated waveguide (SIW) technology," *IEEE Transactions on Antennas and Propagation*, Vol. 63, No. 11, 4640–4647, Nov. 2015.